Interference Analysis in Cooperative Linear Multi-Hop Networks Subject to Multiple Flows

By

Quratulain Shafi

2010-NUST-MS-CSE(S)-28

Supervisor

Dr. Syed Ali Hassan

Department of Electrical Engineering

A thesis submitted in partial fulfillment of the requirements for the degree of Masters in Communication Systems Engineering (MS CSE)

In

School of Electrical Engineering and Computer Science,

National University of Sciences and Technology (NUST),

Islamabad, Pakistan.

(August 2013)

Approval

It is certified that the contents and form of the thesis entitled "**Interference Analysis in Cooperative Linear Multi-Hop Networks Subject to Multiple Flows**" submitted by **Quratulain Shafi** have been found satisfactory for the requirement of the degree.

Advisor: **Dr. Syed Ali Hassan**

Signature: ____________________

Date: ____________________

Committee Member 1: **Dr. Adeel Baig**

Signature: ____________________

Date: ____________________

Committee Member 2: **Dr. Adnan Khalid Kiani**

Signature: ____________________

Date: ____________________

Committee Member 3: **Dr. Zawar Hussain Shah**

Signature: ____________________

Date: ____________________

Abstract

We study the effects of allowing multiple packets to flow simultaneously in a cooperative multi-hop transmission system, where a group of nodes in each hop transmits the same message to another group of nodes in a cooperative manner. Although, the packet delivery rate may increase with multiple packet flows, however, the desired signals of one packet may get interfered with the signals of the other packets in the network; increasing the outage probability at a hop, and thereby causing some of the packets to die off. We analyze this phenomenon by modeling the multi-hop transmission of data packets as a conditional Markov process, followed by the derivation of its transition matrix. The transition matrix incorporates the outage probability, which we obtain by studying the distribution of signal-to-interference ratio as the ratio of two hypoexponential random variables (RVs). Each hypoexponential RV is a sum of independent but non-identically distributed exponential RVs. The resulting distribution is used to calculate the outage probability of a node in a cooperative environment in the presence of desired as well as interfering signals. We then use the model to obtain the network coverage, until which a packet can travel for a given packet delivery ratio constraint and perform numerical simulations to validate the analytical model.

Certificate of Originality

I hereby declare that this submission is my own work and to the best of my knowledge it contains no materials previously published or written by another person, nor material which to a substantial extent has been accepted for the award of any degree or diploma at NUST SEECS or at any other educational institute, except where due acknowledgement has been made in the thesis. Any contribution made to the research by others, with whom I have worked at NUST SEECS or elsewhere, is explicitly acknowledged in the thesis.

I also declare that the intellectual content of this thesis is the product of my own work, except for the assistance from others in the project's design and conception or in style, presentation and linguistics which has been acknowledged.

Author Name: **Quratulain Shafi**

Signature: ____________________

Acknowledgment

I am extremely thankful to Allah Almighty for giving me the will and the strength to help me complete my thesis. I feel humbled to have had the opportunity to study and carry out research at SEECS, NUST.

I am indebted to my supervisor, Dr. Ali Hassan, for his unwavering support and encouragement, his tiring efforts to guide me in the right direction during my research, his attempts at providing me insight into the art of research, and his patience in dealing with me.

I am thankful to my parents for their constant support, encouragement, love and patience throughout my master's degree. I am also grateful to my friends and siblings who believed in my abilities and provided me motivation and inspiration at every step.

Last but not least, I also appreciate the advice and much-needed suggestions by my committee members and advice throughout my thesis phase.

Table of Contents

List of Figures

Chapter 1

Introduction

Since its inception, wireless communication has gone through innumerable technological advances with transmit diversity emerging as one of the most prolific solutions to overcome the ever increasing demand for high data rate and reliable communication in wireless networks. Most dynamic and unstructured networks with distributed sources and destinations are wireless and due to distributed variable interference conditions they suffer from heavy outage and extensive loss of data. A number of diversity schemes have been introduced to overcome this problem, including time diversity, frequency diversity, multiuser diversity and spatial diversity. In order to overcome fading, diversity provides the receiver with multiple, uncorrelated replicas of same signal carrying similar information.

Spatial diversity is the most common diversity technique that uses multiple antennas at the transmitting and receiving end to transfer more data at the same time to improve quality and reliability of a wireless link. This technique is termed as multiple input-multiple output (MIMO) [1] that provides high data rate wireless communication links and high speed links that

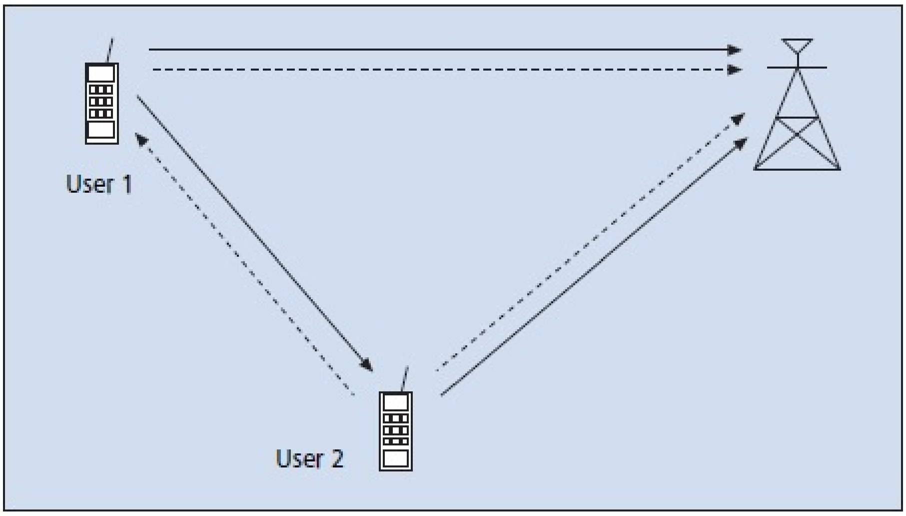

Figure 1.1: Cooperative communication [3]

still offer good Quality of Service (QoS). MIMOs have helped improve the performance and capacity of wireless communications, hence absorbing a lot of research efforts recently. The antennas in MIMOs are made smarter by enabling them to exploit the phenomenon of multipath to combine the information from multiple signals, thus improving speed, data integrity and receiver signal-capturing power. However, the need for multiple antennas makes the network expensive and consumes more space posing limitations on the size of the network [10]. Cooperative communication also termed as distributed multiple input-multiple output (MIMO) systems emerged as a solution to exploit the potential MIMO gains on a distributed scale, where single antenna nodes are used, while utilizing the multiplexing and spatial diversity capability of MIMOs [8]. As shown in Fig. 1.1 each user in a cooperative communication system is supposed to transmit data as well as act as a cooperative agent for another user. When in cooperative mode, it can be said that a user utilizes more power as it is transmitting for both users.

However, diversity reduces the baseline transmit power. Therefore, the goal of a network designer is a net reduction of transmit power, given everything else remains constant. Cooperation gain makes the system more robust, increases user's capacity and can be used to increase cell coverage in a cellular system[5]

The concept of cooperative communication originates from information theoretic properties of the relay channel[4], in which the authors analyze the capacity of the three-node network consisting of a source, a destination, and a relay. The basic idea behind cooperative communication is that of multiple users sharing resources in a network, hence the term user-cooperation. The motivation behind inception of this phenomenon is to provide the nodes in a network the ability to share power and computation, saving overall network resources as a result. User-cooperation strategies are made more applicable when provided with a multi-hop environment that enables rapid deployment with lower-cost backhaul and easy coverage in hard-to-wire areas [7]. Fig. 1.2 shows cooperative diversity where intermediate nodes act as relay nodes and cooperate with source node to transmit data to the destination[2]. In traditional communication networks, information is transferred from one node to another using physical layer only. On the other hand, in user-cooperation, whole network acts as a transmission channel for communication of data. A three-terminal network can be taken as a fundamental unit in user-cooperation, as the existence of more than two communicating terminals makes cooperation possible.

Cooperative diversity can be performed based on different relaying strategies such as: Amplify and Forward (AF), Decode and Forward (DF) and

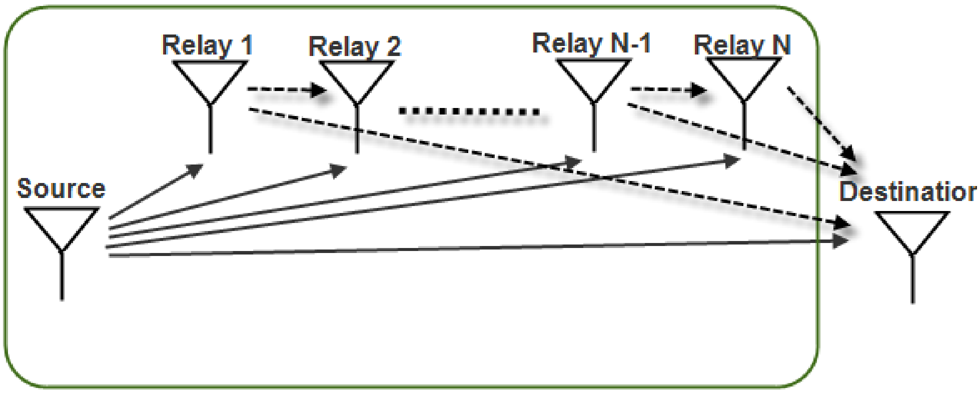

Figure 1.2: Cooperative diversity [4]

coded cooperation. We assume DF nodes that allow the relay node to decode the received noisy signal from the source node, re-encode it and forward it to the destination [3].

In our system model we assume a linear multi-hop cooperative network that has multiple applications in wireless sensor networks including pipeline monitoring or perimeter surveillance, where it is necessary to take measurements at regular intervals along a lengthy piece of infrastructure. In a multi-hop cooperative transmission (CT), the resources of multiple, spatially separated radios are shared to transmit the data of a single source for improving link reliability and providing range extension by achieving transmit diversity [28].

A network can be made more efficient when multiple packet are allowed to flow simultaneously i.e., enabling the user to insert another packet into the network without waiting for the previous packet to reach its destination. The fewer the number of time slots between two packets, more packets can be transmitted in less time, increasing packet delivery rate. However, when multiple packets flow simultaneously they may interfere with each other, resulting in loss of packets and hence reduction in the reliability of the network. Therefore, there is a dire need to model a system that enables multiple packets to flow simultaneously in a cooperative environment with tolerable interference.

1.1 Problem Statement

Cooperative networks can be made more efficient by allowing multiple packets to flow simultaneously, as more packets can be transmitted from the source to the destination in less time. This will eventually increase the packet delivery rate, depending on the value of packet insertion rate (PIR), i.e., the number of time slots that a user waits before sending another packet into the network. Along with the benefits of multi-flow comes the disadvantage of interference; transmission of one packet from one group of nodes to another, acting as a desired signal for one level may end up as an interfering signal for another. This might cause packets to be lost in the way, reducing the quality of service (QoS) of the network, such as the packet delivery ratio (PDR). In addition to other channel impairments, such as path loss and multipath fading, interference plays a vital role in bandlimited cooperative systems and increases the outage probability of a node significantly. Therefore, an accurate model is required that can enable a network designer to observe the amount of interference that can be tolerated for obtaining a certain quality of service and network coverage, as well as to observe the effect of increasing interference on the outage probability, by varying packet insertion rate and tiers of interfering levels. Furthermore, the accuracy of the analytical model needs to be proved by running numerical simulation and comparing them with the analytical results.

1.2 Contribution

We allow the flow of multiple packets simultaneously, in a cooperative linear network, and model the effects of interference that packets might have on each other. In addition to other channel impairments, such as path loss and multipath fading, interference plays a vital role in bandlimited cooperative systems and increases the outage probability of a node significantly. For the purpose of deployment, we make the network flexible by allowing the user to vary the network parameters, which include packet insertion rate, number of interfering tiers, and the number of nodes in each level, contingent upon a required QoS and coverage.

We stochastically model the multi-flow, multi-hop network with a class of absorbing conditional Markov chains and prove numerically that the conditional Markov chain also exhibits a quasi-stationary distribution [30], and that Perron-Frobenius theorem [29] holds for conditional Markov chain if the random process is assumed to be homogeneous.

We derive the outage probability of a node in the presence of desired as well as interfering signals. We assume a Rayleigh fading environment, hence, both the desired and the interfering powers are exponentially distributed. To obtain an expression of the outage probability, the cumulative distribution function (CDF) of the ratio of sum of desired powers and the sum of interfering powers is required.

1.3 Thesis Organization

The rest of the thesis is structured in the following manner. In Chapter 2, we present some background and literature review of modeling in cooperative networks and interference in cooperative networks. Chapter 3 gives a detailed description of the network layout followed by the proposed model of the network using conditional Markov chain and the derivation of its transition probability matrix. In Chapter 4, the accuracy of the model is tested by comparing analytical results with numerical simulations. We conclude by giving an overview of our contributions and possible future work in this particular subject in Chapter 5.

Chapter 2

Literature Review

2.1 Modeling Cooperative Network

Cooperation among mobile users has been proven to increase system throughput, besides making the user's achievable data rates less vulnerable to channel variations [5, 6]. Some type of diversity protection is required as the quality of service and data rate of the mobile users within the duration of the call are limited by the rapid variation in the channel conditions. Increase in the data rate due to cooperation among mobile user can be translated into reduced power for the users. With cooperation, users can achieve a certain rate with less total power, which can extend the battery life of the mobile users. The cooperation gain may also be used to increase cell coverage in a cellular system.

Opportunistic Large Array (OLA)[11], a form of concurrent CT was proposed by Anna Scaglione and Yao-Win Hong, that allows a group of nodes in each hop to transmit the same message to another group of nodes, improving the system performance in terms of diversity and robustness. In an

OLA transmission, the source transmits its message and all neighbouring nodes that can decode the message relay it immediately to next level nodes, and this process continues until the message reaches the destination. It does not require any medium access or routing overhead and each node makes its decision autonomously. Due to the innumerable benefits of OLAs in various areas such as mobile networks and sensor networks, considerable amount of work is present in literature, e.g., [9, 22, 23, 24, 25, 26].

Infinite node density OLA transmissions (with single source packet) were initially studied using Monte-Carlo methods because of the analytical intractability [27]. A model, based on Markov chain has been introduced for multi-hop cooperative linear networks without the *continuum* assumption in [14], however, in this work, new packet is not allowed to be inserted into the network unless the previous packet reaches its destination. Under fading channel environment, the authors modeled the received power on a node as a hypoexponential distribution and provided an upper bound on the network coverage. They modeled the channel as an independent Rayleigh fading channel and path loss with an arbitrary path loss exponent.

2.2 Hypoexponential over Hypoexponential Distribution

Expressions of outage probabilities based on signal-to-interference ratio (SIR) exist in literature for a variety of channel models, including log-normal [15], Rayleigh and Rician [16] fading environments. In all of these cases, a single desired signal is corrupted by many interfering signals, where it is assumed that all the interfering signals have same statistics. On the other hand, in CT-based networks, a node receives several copies of the desired signal. If two or more messages are being propagated simultaneously in the network, then the interference will reduce the SIR at that node, resulting in a higher outage probability. We assume a Rayleigh fading environment, hence, both the desired and the interfering powers are exponentially distributed. To obtain an expression of the outage probability, the cumulative distribution function (CDF) of the ratio of sum of desired powers and the sum of interfering powers is required. This distribution is termed as hypoexponential [21] over hypoexponential distribution. The ratio of functions of various RVs has been introduced in literature including exponential [17] and gamma [18]. However, to the best of the authors knowledge, no such distribution expressing the aforementioned ratio has been derived.

2.3 Interference

In addition to other channel impairments such as path loss and multipath fading, interference plays a vital role in bandlimited cooperative systems and increases the outage probability of a node significantly. Interference due to multi-packet OLA transmission within a single flow is studied, along a disk [12] as well as strip-shaped network [13]. However, in both these works, the authors assume that the sequence converges to a continuum limit, as the number of nodes in the network goes to infinity, known as the *continuum* assumption, which is not appropriate for low density networks. In these works authors analyze the impact of the intra-flow interference in OLA transmission and present the signal model and the properties of spatially pipelined OLA transmission. In strip network, the length is much greater than the width and as opposed to the disk networks, it is feasible to improve the network throughput by inserting a new packet before the previous packet clears the network. The optimal packet insertion period that maximizes the throughput over a finite network without causing packet loss is found numerically, facilitated by upper and lower bounds.

Chapter 3

Modeling

In this chapter, we give a detailed description of our system in Section 3.1 with the assumptions and network parameters followed by the modeling of our network using conditional Markov chains in Section 3.2. Finally The formulation of transition probability matrix is presented in Section 3.3.

3.1 System Description

Consider a linear network topology with decode-and-forward (DF), half-duplex nodes placed d distance away from each other. Each level or hop consists of a fixed number of nodes denoted as M that cooperatively send the message signal to the M nodes of next level as shown in Fig. 1, where $M = 4$. All the nodes that can decode the message, relay the message to the M nodes of the next level and this process continues until the message reaches the destination. We assume that the source node has multiple packets back-logged to be transmitted to the destination. Hence, the network undergoes multiple flows with several packets traversing the network simultaneously.

The source inserts a new data packet into the network and each packet takes one time slot to move from one level to the next. We assume perfect timing synchronization between the nodes of a level. Therefore, all the DF nodes of a level transmit at the same time over orthogonal fading channels. Here, we define two network parameters; i) packet insertion rate (PIR), R, and ii) tiers of interference, T. PIR is defined as the rate per time slot at which the source transmits a new packet. Since we assume half-duplex radios, a full rate transmission, $R = 1$, implies a packet insertion after waiting one time slot. For example, in Fig. 1(a), the DF nodes at level $(n-1)$ transmit packet p_x to level n, where x represents the packet number being transmitted.[1] Similarly, level $(n+1)$ transmits p_{x-1} to level $(n+2)$, and so on. This is an example of *fastest possible* insertion rate.

In Fig. 1(b), $R = 2$ implies that the source transmits a packet after waiting two time slots between consecutive transmissions. Therefore, when level $(n-1)$ transmits p_x to level n, level $(n+2)$ transmits p_{x-1} to level $(n+3)$. Although, the intended destinations of level $(n-1)$ nodes are level n nodes (for any R), however, assuming omnidirectional antennae, the transmissions will be overheard by the neighbouring levels, causing interference. We assume a band-limited system and that all the nodes use the same carrier frequency, thereby causing co-channel inter-flow interference. Solid arrows from level $(n-1)$ to level n show the multiple desired signals, whereas, the dotted arrows represent the unwanted signals that occur because of multiple flows in the network. With different tiers, T, different number of levels interfere with the nodes of a level. As shown in Fig. 1(a), when $T = 1$, the unwanted signals

[1] We have shown transmissions to one node only (namely, the first node of level n). However, all the nodes of level n receive the message from the DF nodes of level $(n-1)$.

affecting the node arrive only from level $(n+1)$, whereas when $T = 2$, levels $(n+3)$ and $(n-3)$ also contribute to the interference with packet insertion rate, $R = 1$. When we increase R, the unwanted signals arrive from levels that are further away from the concerned node as shown in Fig. 1(b) where $R = 2$. Therefore, the interfering levels differ with different combinations of T and R.

At a certain level a node can decode and forward the packet without error when its received desired signal power and signal-to-interference ratio (SIR) are greater than thresholds, α and τ, respectively. The filled black circles in Fig. 1 represent the DF nodes while the hollow circles show that the nodes have not decoded the data. The desired received power at the mth node of level n, denoted as $P_{r_m}(n)$ is given as

$$P_{r_m}(n) = P_t \sum_{k=1}^{K} \frac{\mu_{km}}{(d_{km})^{\beta}}, \tag{3.1}$$

where we assume that the transmit power P_t is constant for all the nodes of the network. The channel gain, μ_{km}, from node k in the previous level to node m in the current level is exponentially distributed with unit mean and corresponds to the squared envelope of the signal undergoing Rayleigh fading. The distance d_{km} represents the Eucledian distance between the nodes and β is the path loss exponent. The summation is over the DF nodes of previous level such that $K \leq M$.

SIR, φ, which is the ratio of desired and interfering power is given as

$$\varphi = \frac{\sum_{k=1}^{K} \frac{\mu_{km}}{(d_{km})^{\beta}}}{\sum_{i=1}^{I} \frac{\mu_{im}}{(d_{im})^{\beta}}}, \tag{3.2}$$

where K and I are the number of desired and interfering signals, respectively. We assume that the interfering signals also exhibit Rayleigh flat fading, where

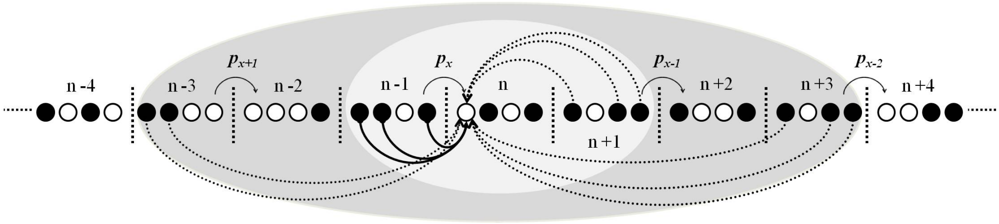

(a) $R = 1$

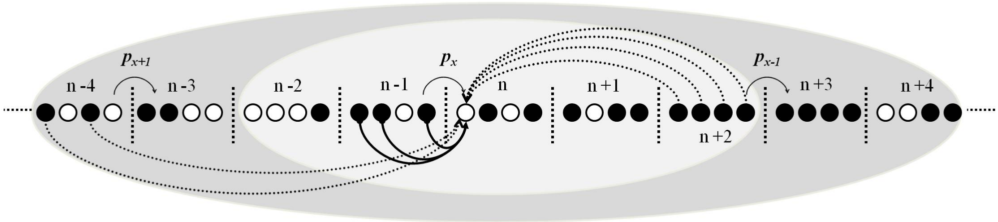

(b) $R = 2$

Figure 3.1: Network topology for PIR 1 and 2, light gray area denotes tier 1 interference and dark gray area denotes additional interfering signals from tier 2.

d_{km} and d_{im} are the distances between the node in the current level and the nodes in the previous and interfering levels, respectively.

3.2 Modeling By Conditional Markov Chain

In this section, we propose the mathematical modeling of the network described in Section 3.1 with a class of discriminative model that forms a linear-chain conditional random field also known as conditional Markov chain [19]. Let $\mathcal{X}(n)$ denotes the state of the network at level n. A straight-forward way to model the state of the system is to represent the number of DF and non-DF nodes at level n. Let $\mathbf{1}_m(n)$ denotes the indicator function of a node m which takes value 1 when node m is a DF node and 0 when the node m

could not decode the data. Hence the state of the system at level n is denoted as $\mathcal{X}(n) = [\mathbf{1}_1(n), \mathbf{1}_2(n), ..., \mathbf{1}_m(n)]$, where $\mathcal{X}(n)$ is an $M-$bit binary word and each outcome is a state consisting of 2^M combinations in decimal form; $0, 1, ..., 2^M - 1$. As discussed previously, a node receives desired as well as interfering signals. Let $\mathcal{Y}$ denotes the set of states that causes interference to the level under consideration. The states in $\mathcal{Y}$ depend on the value of R and T. For example, $\mathcal{Y}$ consists of levels $(n-3)$, $(n+1)$ and $(n+3)$ when $R = 1$ and $T = 1$ as shown in Fig. 3.1(a). It can be shown that the cardinality of $\mathcal{Y}$, given as $|\mathcal{Y}| \leq \infty$ for a given tier, T and PIR, R. Based on these assumptions, the state of the system at level n i.e., $\mathcal{X}(n)$ depends on the previous state $\mathcal{X}(n-1)$ and $\mathcal{Y}$. Hence $\mathcal{X}(n)$ conditional on $\mathcal{X}(n-1)$ and $\mathcal{Y}$ forms a conditional Markov chain [19], such that

$$\begin{aligned} &\mathbb{P}\left\{\mathcal{X}(n) = i_n \,|\mathcal{X}(n-1) = i_{n-1}, ..., \mathcal{X}(1) = i_1, \mathcal{Y}\right\} \\ &\qquad = \mathbb{P}\left\{\mathcal{X}(n) = i_n \,|\mathcal{X}(n-1) = i_{n-1}, \mathcal{Y}\right\}. \end{aligned} \tag{3.3}$$

Here, the conditional Markov chain is homogeneous for a given T and R, with the assumption that for all the hops in the network, the statistics of the channel remains the same. This implies that if we fix R and T, similar system conditions can be observed at a later stage down the network. The PIR is generally fixed in the network. The motivation for fixing T is that we will later show that the increase in interfering tiers follows a diminishing returns phenomenon and considering additional interference tiers do not impact the network performance (e.g., outage probability of a node). This is because, after a sufficiently large T, the interfering levels are far apart from the level under consideration and are not contributing to the interference. It can be seen that all the nodes at a certain level can fail to decode the data successfully, thus forcing the Markov chain to go into an absorbing state (i.e., state 0 in decimal). This will result in the termination of the transmission for a particular packet, p_x. Therefore, the state space of the conditional Markov chain, $\mathcal{X}$, can be denoted as $\{0\} \cup S$, where $S = \left\{1, 2, ..., 2^{M-1}\right\}$, is the finite transient irreducible state space, while 0 is the absorbing state such that $\lim_{n\to\infty} \mathbb{P}\{\mathcal{X}(n) = 0\} \nearrow 1$ a.s.

There always exists a probability for the transition of data from one transient state to another because of the irreducible state space S. We describe the conditional Markov chain in the form of two matrices. The first matrix, $\widetilde{\mathbf{Q}}$, is the full, $2^M \times 2^M$ transition probability matrix representing the states in the set $\{0\} \cup S$. In this matrix each row sums to one. We cross out the columns and rows that involve the transitions to and from state 0 in $\widetilde{\mathbf{Q}}$ to form the second matrix, $\mathbf{Q}$, making a $\left(2^M - 1\right) \times \left(2^M - 1\right)$ submatrix of $\widetilde{\mathbf{Q}}$, that corresponds to the states in S. It can be construed here that the transition probability matrix, $\mathbf{Q}$, is not true stochastic, as its row entries do not sum to 1. Moreover, $\mathbf{Q}$ being a square irreducible non-negative matrix inevitably results in the existence of an eigenvalue, ρ, according to Perron-Frobenius theorem [20] such that, $\{0 < \rho < 1\}$. According to the Markov chains theory, if a certain distribution $\mathbf{u} = (u_i, i \in S)$ is the left eigenvector of the transition matrix, $\mathbf{Q}$, corresponding to ρ, i.e., $\mathbf{uQ} = \rho\mathbf{u}$, $\mathbf{u}$ can be termed as ρ-invariant distribution

As time proceeds, the limiting behaviour of the Markov chain portrays that termination of the transmission of data or in other words killing is an inevitable event, since $\forall n, \mathbb{P}\{\mathcal{X}(n) = 0\} > 0$. However, we require the distribution of the transient states, just before the absorbing state is reached.

This limiting distribution is known as the quasi-stationary distribution of the Markov chain [20]. The quasi-stationary distribution is provided by the ρ-invariant distribution for one-step transition probability matrix of the Markov chain on S for which, we first calculate the *maximum* eigenvector, $\hat{\mathbf{u}}$, of $\mathbf{Q}$. Defining $\mathbf{u} = \hat{\mathbf{u}} / \sum_{i=1}^{2^M - 1} \hat{\mathbf{u}}_i$, as a normalized version of $\hat{\mathbf{u}}$ that sums to one gives the quasi-stationary distribution of $\mathcal{X}$. Hence the unconditional probability of being in state r at level n is given as

$$\mathbb{P}\left\{\mathcal{X}\left(n\right) = r\right\} = \rho^n u_r, \quad r \in S, \;\; n \geq 0. \tag{3.4}$$

The time at which the killing occurs is represented as $E = \inf\left\{n \geq 0 : \mathcal{X}(n) = 0\right\}$. Therefore,

$$\mathbb{P}\left\{E > n + n_0 | E > n\right\} = \rho^{n_0}, \tag{3.5}$$

while the quasi-stationary distribution of the Markov chain is given as

$$\lim_{n \to \infty} \mathbb{P}\left\{\mathcal{X}(n) = r | E > n\right\} = u_r, \quad r \in S. \tag{3.6}$$

3.3 Formulation of Transition Probability Matrix

The state transition probability matrix, $\mathbf{Q}$, and its detailed formulation is presented in this section. It is further shown that the eigenvector of the state transition probability matrix can be used to find the quasi-stationary distribution. The probability for a node m to decode at level n is

$$\begin{aligned} \mathbb{P}\left\{\text{node}\, m \,\text{of level}\, n \,\text{will decode}\right\} &= \mathbb{P}\left\{\mathbb{I}_m\left(n\right) = 1\right\} \\ &= \mathbb{P}\left\{P_{r_m}\left(n\right) \geq \alpha \;\cap\; \varphi_m\left(n\right) \geq \tau\right\}, \end{aligned} \tag{3.7}$$

where $P_{r_m}(n)$ and $\varphi_m(n)$ represent the received power and the received SIR respectively, for the mth node at level n. The success probability of the node is given as

$$\begin{aligned} &\mathbb{P}\left\{P_{r_m}(n) \geq \alpha \, \cap \, \varphi_m(n) \geq \tau\right\} \\ &= \int_{x=\alpha}^{\infty} \left[\int_{y=0}^{x/\tau} f_{\varphi_m}(y)dy\right] f_{Pr_m}(x)dx, \end{aligned} \tag{3.8}$$

where $f_{Pr_m}(x)$ and $f_{\varphi_m}(y)$ are the probability distribution functions (PDFs) of the received power and the received SIR at the mth node, respectively. The nodes exhibit a performance threshold, where data received at a certain node is decoded successfully only when both the received power, P_r, and SIR, φ, exceed certain defined thresholds, denoted by α and τ, respectively. Assuming a Rayleigh fading environment, both the desired and the interfering powers are exponentially distributed. Hence the numerator of (3.2) represents a random variable which is a sum of K independent but non-identically distributed (i.n.i.d) exponential RVs. Same phenomenon goes for the denominator of (3.2). The resulting distribution for the sum of K desired powers and for the sum of I interfering powers are both hypoexponential distributions [21] as given in the following definition.

Definition 1. A RV $X \sim$ hypoexponential $(\boldsymbol{\lambda})$ with positive parameter vector $\boldsymbol{\lambda} = \lambda_1, \lambda_2, ..., \lambda_k$, such that $\lambda_k \neq \lambda_j$, if X is a sum of mutually independent exponential RVs, $X_1, X_2, ..., X_k$ with respective parameters $\lambda_1, \lambda_2, ..., \lambda_k$.

To obtain an expression of the outage probability, the cumulative distribution function (CDF), $F_Z(z)$, of the ratio of sum of desired powers and the sum of interfering powers is required, which is derived in the following theorem.

Theorem 1 (**Ratio of independent hypoexponential random variables**)**.** *Let* $X \sim$ *hypoexponential* $(\boldsymbol{\lambda})$ *and* $Y \sim$ *hypoexponential* $(\boldsymbol{\eta})$ *be two independent hypoexponential RVs and let* $Z = X/Y$*. The complementary cumulative distribution function (CCDF) of* Z *is given as*

$$\mathbb{P}\{Z > \tau\} = \sum_{i=1}^{I}\sum_{k=1}^{K} C_i D_k \left(\frac{\lambda_k}{\tau\eta_i + \lambda_k}\right), \tag{3.9}$$

where

$$C_i = \prod_{j=1, j\neq i}^{I} \frac{\eta_i}{\eta_i - \eta_j},\ D_k = \prod_{l=1, l\neq k}^{K} \frac{\lambda_k}{\lambda_k - \lambda_l}. \tag{3.10}$$

Proof. Each X and Y is a sum of independent exponential RVs, such that

$$X = X_1 + X_2 + X_3 + ... + X_K, \tag{3.11}$$

$$Y = Y_1 + Y_2 + Y_3 + ... + Y_I. \tag{3.12}$$

As X_k and Y_i both have exponential distribution, hence

$$f_\zeta(u) = \frac{1}{\phi} exp\Big(\frac{-u}{\phi}\Big), \tag{3.13}$$

where $\zeta \in \{X_k, Y_i\}$ with respective parameters $\phi \in \{\lambda_k, \eta_i\}$ such that $\lambda_k \neq \eta_i$, $\forall_{i,k}$. The hypoexponential distribution of X in (3.11) is given as

$$f_X(x) = \sum_{k=1}^{K} D_k \frac{1}{\lambda_k} exp\Big(\frac{-x}{\lambda_k}\Big), \tag{3.14}$$

Similarly, the distribution of Y in (3.12) is also hypoexponential as given in (3.14) with λ_k replaced with η_i and D_k with C_i. Since X and Y are independent, the CDF of the ratio of $Z = X/Y$ is obtained by integrating the original PDFs on the region of support, i.e.,

$$\mathbb{P}\{Z \leq \tau\} = 1 - \mathbb{P}\{Z > \tau\} = 1 - \mathbb{P}\{X/Y > \tau\}. \tag{3.15}$$

Therefore,

$$\mathbb{P}\{X/Y > \tau\} = \int_{x=0}^{\infty} \left[\int_{y=0}^{x/\tau} f_Y(y)dy \right] f_X(x)dx, \tag{3.16}$$

The term under square brackets is the CDF of hypoexponential RV and is given as

$$\int_{y=0}^{x/\tau} f_Y(y)dy = \sum_{i=1}^{I} C_i \left[1 - exp\Big(- \frac{x}{\tau\eta_i} \Big) \right]. \tag{3.17}$$

By combining (3.14) and (3.17), (3.16) is evaluated as

$$\mathbb{P}\{Z > \tau\} = \sum_{i=1}^{I} \sum_{k=1}^{K} C_i D_k \left(\frac{\lambda_k}{\tau\eta_i + \lambda_k} \right). \tag{3.18}$$

■

Now we are in a position to derive the success probability of a node given by (3.7), where we assume that the received power, P_r is required to be greater than α, which requires changing the lower limit of x in (3.16) to α. Thus the probability of success is given as

$$\mathbb{P}\{Z > \tau\} = \sum_{i=1}^{I} \sum_{k=1}^{K} \frac{C_i D_k}{\lambda_k} \int_{x=\alpha}^{\infty} \left[exp\Big(\frac{-x}{\lambda_k}\Big) - exp\Big(\frac{-x}{\lambda_k} - \frac{-x}{\tau\eta_i}\Big) \right] dx, \tag{3.19}$$

which after a straight-forward analysis gives

$$\mathbb{P}\{Z > \tau\} = \sum_{i=1}^{I} \sum_{k=1}^{K} C_i D_k exp\left(\frac{-\alpha}{\lambda_k}\right) \left[1 - \frac{\tau\eta_i}{\tau\eta_i + \lambda_k} exp\left(\frac{-\alpha}{\tau\eta_i}\right) \right]. \tag{3.20}$$

Until now, the number of interfering nodes are represented by I, where $I \in \mathbb{Z}^+$, $\mathbb{Z}^+$ being the set of positive integers. However, in the network of Fig. 3.1, the number of interfering nodes depends upon R and T. Hence, we represent an interfering level as $(n+\gamma_j)$ where $\gamma_j \in \Gamma$ and $j \in \{1,2,...,|\Gamma|\}$, where $|\Gamma|$ is the cardinality of set Γ. The set Γ depends on the values of R and T, such that $\Gamma = \{1\}$ when $R = 1$ and $T = 1$, whereas $\Gamma = \{1, 3, -3\}$ when $R = 1$ and $T = 2$ as shown in Fig. 3.1. We define two sets, $\mathbb{K}$ and $\mathbb{I}$, to represent the indices of the nodes that are active in the desired and interfering levels, respectively, where $|\mathbb{K}| \le M$. However, as $|\Gamma| \ge 1$, there might be different indices for each interfering level, making $|\mathbb{I}| \le M|\Gamma|$. We can now express, the probability of success of the mth node at level n as

$$P_s^{(m)} = \sum_{\substack{i\in\mathbb{I}_{\left(n+\gamma_j\right)},\\ \gamma_j\in\Gamma}} \sum_{k\in\mathbb{K}_{(n-1)}} C_i D_k exp\left(\frac{-\alpha}{\lambda_k^{(m)}}\right) \left[1 - \frac{\tau\ \eta_{i,\gamma_j}{}^{(m)}}{\tau\ \eta_{i,\gamma_j}{}^{(m)} + \lambda_k^{(m)}} exp\left(\frac{-\alpha}{\tau\ \eta_{i,\gamma_j}{}^{(m)}}\right)\right], \tag{3.21}$$

where C_i and D_k are given in (3.10), $\lambda_k^{(m)}$ is the coefficient of the exponential RV from node k in the desired level $(n-1)$ to node m in the current level n, and $\eta_{i,\gamma_j}^{(m)}$ is the coefficient of the exponential RV from node i in the interfering level $(n+\gamma_j)$ to the mth node in the current level n given as

$$\lambda_k^{(m)} = \frac{1}{d^\beta (M-k+m)^\beta}, \tag{3.22}$$

and

$$\eta_{i,\gamma_j}^{(m)} = \begin{cases} \gamma > 0, & \frac{1}{d^\beta (M|\gamma_j|-m+i)^\beta} \\ \gamma < 0, & \frac{1}{d^\beta (M|\gamma_j|-i+m)^\beta}. \end{cases} \tag{3.23}$$

We represent the states of the desired level, $(n-1)$ and current level, n as s_1 and s_2 such that $\{s_1, s_2\} \in S$. The state of interfering levels, on the other hand belongs to $\{0\} \cup S$, as there is a possibility that all the nodes in an interfering level fail to decode data from their respective desired levels, causing no interference for the level under consideration. For a given R and T, we have $|\Gamma|$ interfering levels, hence the total possible number of combinations of interfering level states become $\left(2^M\right)^{|\Gamma|}$. If we assume that all the interfering levels are equally likely, the transition probability will be an average of all the probabilities over all the combinations of interfering level states. If we let the indices of those nodes that decode the data correctly in state s_2 (at level n) and indices of those that fail to decode, to be $\mathbb{N}_n^{(s_2)}$ and $\overline{\mathbb{N}}_n^{(s_2)}$, respectively, the probability, P_ϑ for interfering combination ϑ is given as

$$P_\vartheta = \prod_{m \in \mathbb{N}_n^{(s_2)}} \left(P_s^{(m)}\right) \prod_{m \in \overline{\mathbb{N}}_n^{(s_2)}} \left(1 - P_s^{(m)}\right), \tag{3.24}$$

where $P_s^{(m)}$ is given in (3.21) and the combination ϑ dictates the set $\mathbb{I}$. Finally, we deduce one-step transition probability for going from state s_1 to state s_2 given interfering set $\mathbb{A}$, where $\mathbb{A}$ represents all possible combinations of interfering levels as

$$P_{s_2|s_1,\mathbb{A}} = \sum_{\vartheta \in \mathbb{A}} \frac{P_\vartheta}{\left(2^M\right)^{|\Gamma|}}. \tag{3.25}$$

The state transition probabilities are used to formulate a $\left(2^M - 1\right) \times \left(2^M - 1\right)$ matrix, $\mathbf{Q}$. The eigenvector of $\mathbf{Q}$ will give us the quasi-stationary distribution.

Chapter 4

Results

In this chapter, we present various results pertaining to the performance of the cooperative network under multiple flows. First of all we present the analytical as well as numerical simulation results to show the validity of Theorem 1, i.e., the ratio of independent hypoexponential RVs. We assume the network topology as shown in Fig. 3.1, to compare the results of the CDF, $\mathbb{P}\{Z < \tau\}$, for $M = 2$ and $R = 1$. It can be seen in Fig. 4.1 that the analytical and numerical results match closely for both the tiers. The analytical results are obtained from (3.9) and the solid curve shows the outage probability (i.e., the CDF) of a single node (specifically the first node of level n) in the presence of desired as well as interfering signals. For a fixed τ, the outage probability increases when we move from tier 1 to tier 2, as tier 2 introduces more interfering signals to the node under consideration. In all the results, we set $d = 1$ and $\beta = 2$.

Fig. 4.2 shows the comparison of distribution of states for analytical and simulation model for $M = 2$, $R = 1$ and $T = 1$, with $\alpha = 0.1$ and $\tau = 0.05$ for various number of hops. When $M = 2$, there are potentially

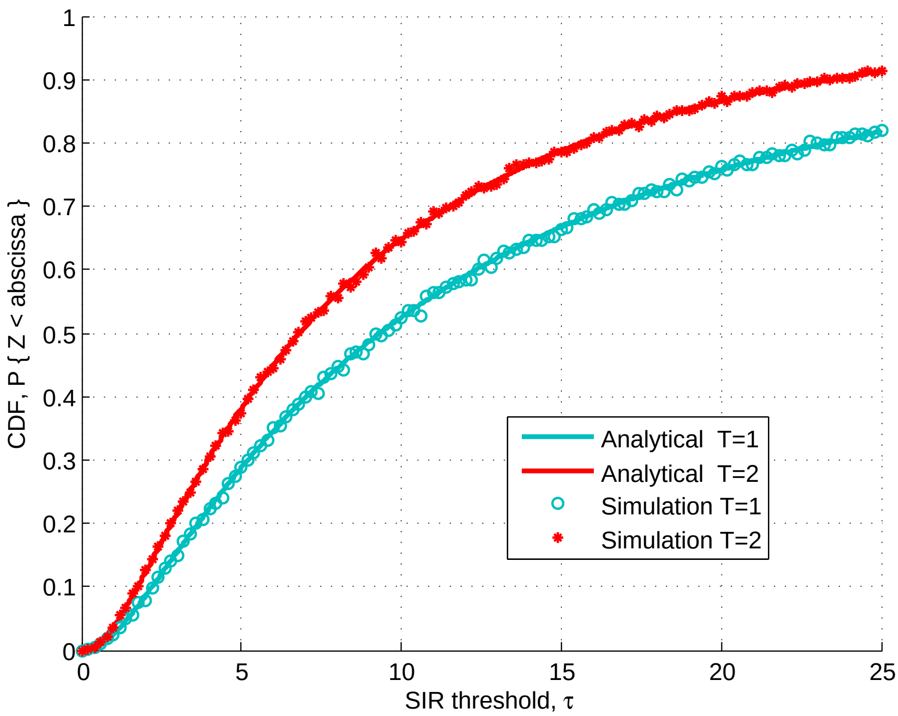

Figure 4.1: CDF of the ratio of two hypoexponential RVs for $M = 2$, $R = 1$.

three transient states in the system, which are $\{0,1\}$, $\{1,0\}$ and $\{1,1\}$. The figure represents the probability of being in each state using the analytical as well as the simulation model. The analytical part is attained using (3.25), whereas for the simulation results, we randomly generate the states initially and then assign 1 or 0 to each node of the next level, if the received power and SIR are greater or less than the thresholds α and τ, respectively. This process continues until all the nodes fail to decode in a level (i.e., the absorbing state is reached). We then take the average of 100,000 simulation trials. It can be noted that with the increase in the number of hops, the probability of each transient state also decreases, however the skewness of all the three

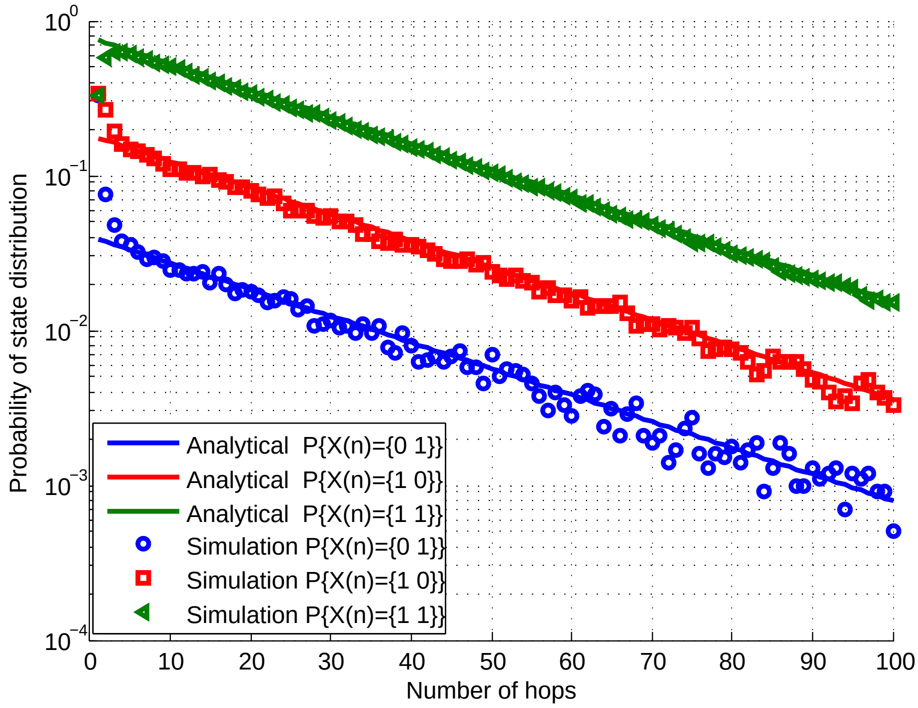

Figure 4.2: Distribution of the states for $M = 2$, $R = 1$, $T = 1$, $\alpha = 0.1$, $\tau = 0.05$.

curves remains constant. This plot shows that the quasi-stationary property is exhibited by the conditional Markov chains. It can be noted that initially the possibility of state distribution is equally likely for the simulation results, i.e., 1/3. However, after a few hops, the network achieves the quasi-stationary distribution for a given R and T.

The probability of one-hop success, ρ, is the Perron-Frobenius eigenvalue of the matrix $\mathbf{Q}$ that represents the probability of at least one node decoding the data. Fig. 4.3 represents ρ versus SIR threshold, τ for various tiers of interfering signals, where $\alpha = 0.05$ and $M = 2$. For a certain τ, the proba-

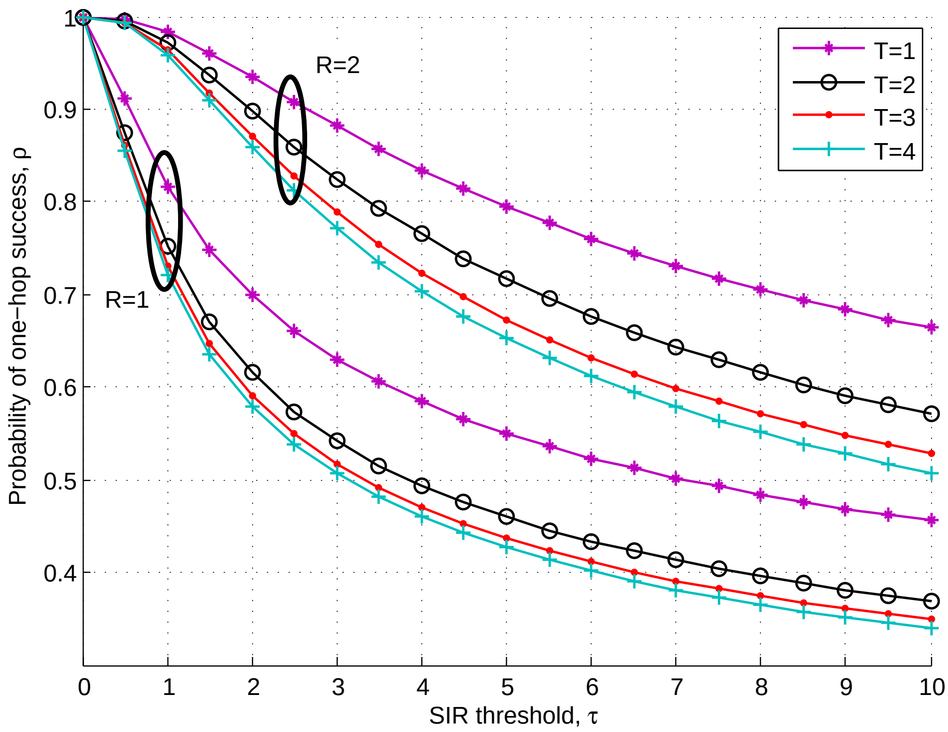

Figure 4.3: Probability of one-hop success for $M = 2$, $\alpha = 0.05$.

bility of one-hop success decreases when we move from $T = 1$ to $T = 2$, and similarly for $T = 2$ to $T = 3$ and so on, as more interfering signals are introduced. However, the effect of increasing interference tiers show diminishing returns. Therefore, for this network topology, the effect of interference on the performance of a node is noticeable for upto two-tierd levels of interference only. Same effect can be seen for $R = 2$, with the exception that this case shows better success probability for a fixed τ. This is because when PIR is higher, the interfering tiers are spread further apart resulting in a reduced outage probability.

The quality of service (QoS), η of this type of network can be represented as the probability of not having entered the absorbing state, making its ideal value 1. Equation (3.4) provides the maximum number of hops, h, that a packet can travel for a given η, i.e., $\rho^h \geq \eta$, which gives $h \leq \frac{ln\,\eta}{ln\,\rho}$. If the required QoS is decreased, the coverage of the network increases as shown in Fig. 4.4, in which we show the analytical and simulation results for τ versus the number of hops, h that can be reached, which specifies the number of level until which the packet travels with a packet delivery rate (PDR) of η. In Fig. 4.4, $M = 2$, $R = 1$, $T = 1$ and $\alpha = 0.01$. For the simulation results, we run the simulation for 100,000 packets and observe the hop number at which the packet delivery ratio equals the value of η. It can be seen that the analytical model fits the numerical simulations.

Fig. 4.5 shows the distance that can be covered over a range of required SIR threshold, τ, for various values of PIRs and M, where $\alpha = 0.01$. The distance is represented as normalized distance, which is evaluated by multiplying the number of hops, h, and the number of nodes in a certain level, M, and then dividing by d. Higher value of R shows that the network waits for more time slots before inserting another packet, reducing the interference at a certain level for a given tier ($T = 1$ in this case), providing larger network coverage. The lower the value of R, the better is the throughput of the network, as more packets can be transmitted simultaneously, however the desired signal of one packet may interfere with the transmission of other packets causing some of the packets to be lost in the way. Therefore, to attain a certain QoS, a trade off between the two is required. As we increase the number of nodes in each hop, better coverage can be attained for a certain value of τ, indicating the effects of increased diversity gain. It can be

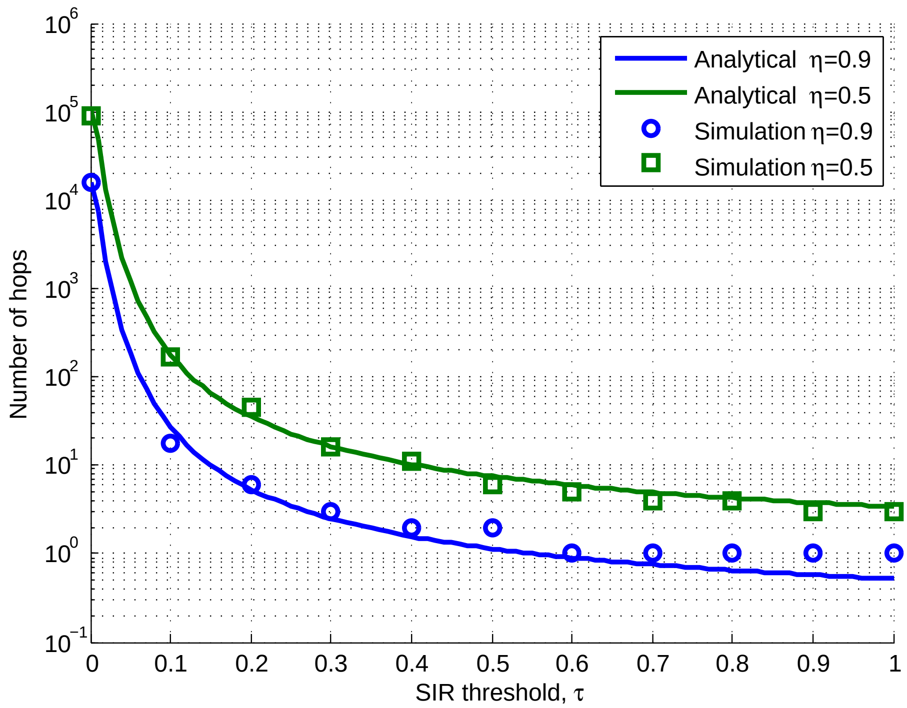

Figure 4.4: Number of hops for $M = 2$, $R = 1$, $T = 1$, $\alpha = 0.01$.

further observed that same distance might be achieved for various combinations of M and R. For instance, at $\tau = 0.4$, same coverage of the network can be achieved if $M = 4$, $R = 2$ or $M = 3$, $R = 3$. The former case has a higher throughput and less delay (owing to larger hop distance) and may be preferred over the latter case.

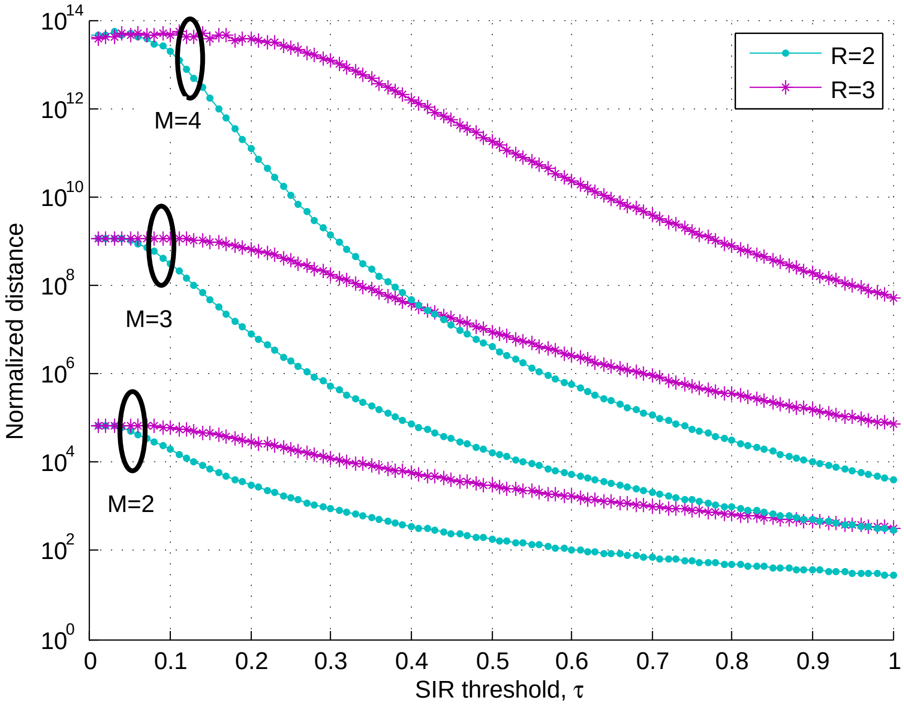

Figure 4.5: Coverage of network for $T = 1$, $\alpha = 0.01$, $\eta = 0.9$.

Chapter 5

Conclusion and Future Work

5.1 Conclusion

Interference due to multiple flows in a cooperative linear network is modeled using conditional Markov chain, where the desired and interfering signals are non-identical and exponentially distributed. Expression for the outage probability based on received power and received signal-to-interference ratio is derived, by determining the CDF of the ratio of two hypoexponential RVs. It is further proven that Perron-Ferobenius theorem can be held true for conditional Markov chain as well, allowing the network to exhibit quasi-stationary distribution. Analytical and simulation results are presented to show the accuracy of the proposed model, as well as to observe the effect of increasing interference on the outage probability, by varying packet insertion rate and tiers of the interference. Therefore, this can eventually enable a network designer to observe the amount of interference that can be tolerated for obtaining a certain quality of service and network coverage.

5.2 Future Directions

A possible future work is to incorporate multiple flows in the model and study the interference-limited performance of the network. The network model can be extended to a two-dimensional grid network. The non-overlapping assumption of our model can be relaxed and an overlapping level of nodes can be considered. A future work may be to study the random deployment of nodes. Synchronization among group of nodes is also an open area of research.

Bibliography

[1] G. J. Foschini and M. J. Gans, "On limits of wireless communications in a fading environment when using multiple antennas," *Wireless Pers. Commun.,* vol. 6, no. 3, Mar 1998, pp. 331-335

[2] J. N. Laneman, D. N. C. Tse, and G. W. Wornell, "Cooperative diversity in wireless networks: Efficient protocols and outage behavior," *IEEE Trans. Inf. Theory*, vol. 50, pp. 3062-3080, Dec. 2004.

[3] A. Nosratinia, E. Todd E and A. Hedayat, "Cooperative communication in wireless networks," *IEEE Commun. Mag*, vol. 42, pp74-80, 2004

[4] T. M. Cover and A. A. E. Gamal, "Capacity Theorems for the Relay Channel," IEEE Trans. Info. Theory, vol. 25, no. 5, Sept. 1979, pp. 57284.

[5] A. Sendonaris, E. Erlip. and B. Aazhang, "User cooperation diversity-part I: system description,*IEEE Trans. Commun.*, vol. 51, no. 11, pp. Nov. 2003.

[6] A. Sendonaris, E. Erlip. and B. Aazhang, "User cooperation diversity-part II: implementation aspects and performance analysis,*IEEE Trans. Commun.*, vol. 50, no. 11, pp. Nov. 2003.

[7] D. Wübben, "Cooperative communication in multihop networks," (Universitt Bremen), [online] 2012, http://www.ant.uni-bremen.de/en/projects/multihop/ (Accessed: 12 December, 2012)

[8] S. Ma, Y. Yang, and H. Sharif "Distributed MIMO technologies in cooperative wireless networks," *Advances in Cooperative Wireless Networking, IEEE Communication Magazine*, May 2011.

[9] A. Kailas and M. A. Ingram, "Alternating opportunistic large arrays in broadcasting for network lifetime extension," *IEEE Trans. Wireless Commun.*, vol. 8, no. 6, pp. 2831-2835, June 2009.

[10] B. S. Mergen, A. Scaglione, and G. Mergen, "Asymptotic analysis of multi-stage cooperative broadcast in wireless networks," *IEEE Trans. Inform. Theory*, vol. 52, no. 6, pp. 2531-2550, 2006.

[11] A. Scaglione and Y. W. Hong, "Opportunistic large arrays: cooperative transmission in wireless multihop ad hoc networks to reach far distances," *IEEE Trans. Sig. Proc.*, vol. 51, no. 8, pp. 2082-2092, 2003.

[12] H. Jung and M. A. Ingram, "Analysis of spatial pipelining in Opportunistic Large Array broadcasts," *in Proc IEEE MILCOM*, pp. 991-996, 2011.

[13] H. Jung and M. A. Ingram, "Analysis of intra-flow interference in opportunistic large array transmission for strip networks," *in Proc. IEEE ICC*, pp. 104-108, 2012.

[14] S. A. Hassan and M. A. Ingram, "A quasi-stationary Markov chain model of a cooperative multi-hop linear network," *IEEE Trans. Wireless Commun.*, vol. 10, no. 7, pp. 2306-2315, 2011.

[15] G. L. Stüber, *Principles of Mobile Communication*, Springer New York, 2011.

[16] Y. D. Yao and A. U. H. Sheikh, "Outage probability analysis for microcell mobile radio systems with cochannel interferers in Rician/Rayleigh fading environment," *Electron. Lett.*, vol. 26 no. 13, pp. 864-866, 1990.

[17] A. Annavajjala, A. Chockalingam and S. K. Mohammad, "On ratio of functions of exponential random variables and some applications," *IEEE Trans. Commun.*, vol. 58, no. 11, pp. 3091-3097, 2007.

[18] R. Kwan and C. Leung, "Gamma variate ratio distribution with application to CDMA performance analysis," *IEEE/Sarnoff Symposium on Advances in Wired and Wireless Communication*, pp. 188-191, 2005.

[19] M. Sinn and B. Chen, "Central limit theorems for conditional markov processes," *J. Machine Learning Research*, vol. 31, pp. 554-562, 2013.

[20] E. Senta, *Non-Negative Matrices and Markov Chains*, 2nd edition, Springer New York, 2006.

[21] S. M. Ross, *Introduction to Probability Models*, 9th edition, Academic Press, 2007.

[22] S. A. Hassan and M.A. Ingram, "On the modeling of randomized distributed cooperation for linear multi-hop networks," in *IEEE Intl. Conf. Commun. (ICC)*, Ottawa, Canada, June 2012.

[23] S. A. Hassan and M. A. Ingram, "A stochastic approach in modeling cooperative line networks," in *IEEE Wireless Commun. Networking Conf. (WCNC),* Cancun, Mexico, March, 2011.

[24] S. A. Hassan, P. Wang, "Dual relay communication system: Channel capacity and power allocations, in *10th IEEE Intl. Wireless and Microwave Techn. Conf. (WAMICON)*, Clearwater, Fl., April 2009.

[25] S. A. Hassan, P. Wang, Y. G. Li, "Equalization for symmetrical cooperative relay scheme for wireless communications," in *11th IEEE Radio and Wireless Symposium (RWS)*, San Diego, CA, Jan. 2009.

[26] P. Wang, S. A. Hassan, Y. G. Li, "A symmetrical cooperative diversity approach for wireless communications," in *th IEEE Intl. Conf. on Circuits and Systems Commun. (ICCSC),* Beijing, China, May 2008.

[27] B. S. Mergen and A. Scaglione, "A continuum approach to dense wireless networks with cooperation," in *Proc. IEEE INFOCOM*, pp. 2755-2763, Mar. 2005.

[28] S. A. Hassan, "Range extension using optimal node deployment in linear multi-hop cooperative networks," in *IEEE Radio and Wireless Symposium (RWS)*, Austin, Texas, Jan. 2013.

[29] C.D Meyer, *Matrix Analysis and Applied Linear Algebra,* SIAM publishers, 2001.

[30] E. A. van Doorn and P. K. Pollett, "Quasi-stationary distributions for reducible absorbing Markov chains in discrete time," *J. Markov Processes and Related Fields*, vol. 15, no. 2, pp. 191-204, 2009.